Toxicology Letters 208 (2012) 115–124

Contents lists available at SciVerse ScienceDirect

Toxicology Letters

journal homepage: www.elsevier.com/locate/toxlet

Short term inhalation toxicity of a liquid aerosol of CdS/Cd(OH)$_2$ core shell quantum dots in male Wistar rats

L. Ma-Hock[a], S. Brill[a], W. Wohlleben[b], P.M.A. Farias[c,d], C.R. Chaves[c,d], D.P.L.A. Tenório[c,d], A. Fontes[e], B.S. Santos[f], R. Landsiedel[a], V. Strauss[a], S. Treumann[a], B. van Ravenzwaay[a,*]

[a] BASF SE, Experimental Toxicology and Ecology, 67056 Ludwigshafen, Germany
[b] BASF SE, Polymer Physics, 67056 Ludwigshafen, Germany
[c] Research Group on Nanostructures and Biological Interfaces; Federal University of Pernambuco (UFPE), 50670-901 Recife, Brazil
[d] Graduate Program on Materials Science, Federal University of Pernambuco (UFPE), 50670-901 Recife, Brazil
[e] Graduate Program on Biological Sciences, Federal University of Pernambuco (UFPE), 50670-901 Recife, Brazil
[f] Graduate Program on Pharmaceutical Sciences, Federal University of Pernambuco (UFPE), 50670-901 Recife, Brazil

ARTICLE INFO

Article history:
Received 22 July 2011
Received in revised form 12 October 2011
Accepted 13 October 2011
Available online 20 October 2011

Keywords:
Quantum dots
Rat
Inhalation
Cadmium
Sub-acute toxicity

ABSTRACT

Colloidal quantum dots (QD) show great promise as fluorescent markers. The QD used in this study were obtained in aqueous medium rather than the widely used colloidal QD. Both methodologies used for the production of QD are associated with the presence of heavy metals such as cadmium (Cd). Here we investigate the short-term inhalation toxicity of water-soluble core-shell CdS/Cd(OH)$_2$ QD. Male Wistar rats were head-nose exposed for 6 h/day on 5 days at the technically maximum concentration (0.52 mg Cd/m^3). Histological examination was performed directly after the last exposure. Additional rats were used for Cd organ burden determinations. Clinical parameters in blood, bronchoalveolar lavage fluid and lung tissue were determined 3 days after the last exposure. To analyze the reversibility or progression of effects, the examinations were performed again after a recovery period of 3 weeks. The results of the study indicate that CdS/Cd(OH)$_2$ QD caused local neutrophil inflammation in the lungs that partially regressed after the 3-week recovery period. There was no evidence that QD were translocated to the central nervous system nor that a systemic acute phase response occurred.

1. Introduction

Quantum dots (QD), first developed in the early 1980s, are crystalline semiconducting nanoparticles comprised of a metalloid crystalline core and a "cap" or "shell" that shields the core, minimizes surface traps and increases quantum yield (Powell and Kanarek, 2006). Cadmium (Cd)-containing QD consist of different core/shell structures: CdS/Cd(OH)$_2$, CdSe/CdS, CdTe/CdS. They are nanoparticles in the low nanometer range, their flouroscence wavelength is closely related to their size. Photobleach tendency of such QDs is low. These properties make them suitable for fluorescent probing applications to detect cancer biomarkers *in vitro* and *in vivo* in cells/tissues/whole body (Gao et al., 2004; Farias et al., 2006). The increasing use and applications of QD in distinct technological areas, however, will invariably result in human exposure to QD.

Beside all their exciting optical and electrical properties, QD are nanoparticles with unknown *in vivo* toxicological properties. Thus, the risk/benefit ratio for the use of nanomaterials in any technological or medical development must be evaluated (Thomas and Sayre, 2004; Medina et al., 2007). For certain medical applications besides intravenous (i.v.) injection inhalation is also a relevant exposure route. Nanoparticles can induce increased lung toxicity compared to larger particles with the same chemical composition at equivalent mass concentration (Oberdörster et al., 2005). In addition, it has been shown that nanomaterials can induce inflammatory reactions in the lungs of experimental animals (Brown et al., 2001; Gilmour et al., 2004; Dailey et al., 2006). Although inflammatory reactions in the lung seem to be a common denominator, the extent of the toxicity induced by nanomaterials depends on a combination of parameters. Among these, the chemical composition and surface modification, size and shape, persistence and the release of metal ions are considered to be the most relevant (Landsiedel et al., 2010). Furthermore, a few of the inhaled nanoparticles could possibly avoid normal phagocytic defenses in the respiratory system and translocate to the blood stream or even to the central nervous system (Kreyling et al., 2002; Oberdörster et al., 2004). In addition to the general toxicity of nanoparticles, it should be noted that intake of QD poses a risk of systemic exposure to Cd. Cd is known to have a biological half-life of 15–20 years in humans

* Corresponding author. Tel.: +49 621 60 5 64 19; fax: +49 621 60 5 81 34.
E-mail address: bennard.ravenzwaay@basf.com (B. van Ravenzwaay).

0378-4274/$ – see front matter © 2011 Elsevier Ireland Ltd. All rights reserved.
doi:10.1016/j.toxlet.2011.10.011

and thus bioaccumulates. It can cross the blood-brain barrier and placenta, and may be systemically distributed to all tissues, with liver and kidney being target organs of toxicity (Hardman, 2006). At this time the vast majority of scientific papers dealing with the toxicity of QD are limited to *in vitro* cytotoxicity assays. A good overview is provided by Pelley et al. (2009). The biological effect caused by Cd-containing QD cannot be covered by *in vitro* assays, especially not their fate. Thus the major purpose of this study was to investigate the potential *in vivo* toxicity of QD using a dose of the maximum technically achievable atmospheric concentration. The QD we investigated were composed of a CdS core surrounded by a $Cd(OH)_2$ shell. We used a 5-day inhalation model (Ma-Hock et al., 2009) to evaluate the effect of QD in rats on the respiratory tract and kidney as target organ for Cd ions. To examine whether free Cd ions became systemically available, urine was examined for QD.

This short-term inhalation study is a screening study. As stated in our previous paper (Ma-Hock et al., 2009), due to the broad spectra of endpoint examined, this type of study provides not only information concerning local toxicity on the respiratory tract but also give indication of systemic toxicity, and provides data for potential body distribution. Due to the sensitive parameters used, it has certain predictivity for potential effect after sub-chronic exposure. Depending on the further development of the material, studies with longer exposure duration may follow.

2. Materials and methods

2.1. Test material and characterization

The test material was an aqueous suspension of QD, composed of a CdS core and surrounded by a $Cd(OH)_2$ shell. The stock suspension had a QD concentration of 140 mg/L. The test material was synthesized by the Research Group on Nanostructures and Biological Interfaces (NIB), UFPE, Recife, PE, Brazil, and used in the unchanged (unpurified) state. The QD were characterized using UV/vis absorption and emission spectroscoscopy. Absorption spectroscopy showed absorption bands at 250 nm and 450 nm, while emission spectroscopy presented a maximum fluorescence peak at 480 nm (full width at half maximum, FWHM = 50 nm). The Cd and sulfur (S) content of the test material as such and specifically the Cd content in the aqueous supernatant after removal of the particles (by ultracentrifugation) were analyzed by inductively coupled plasma optical emission spectrometry (ICP-OES). We found Cd ions in the supernatant at a level of 10 ± 1 ppm. Quantitative analysis of traces and contaminants was performed using X-ray photoelectron spectroscopy (XPS), in excellent agreement with energy dispersive X-ray spectroscopy (EDXS) of the particle fraction: indeed oxygen (O), Cd and S are the dominating elements, and the chemical shift of photoelectron signals from Cd confirms the existence of the passivation layer by the roughly equal presence of binding states of CdS and $Cd(OH)_2$. However, a substantial concentration of carbon (C) was identified: when the QD suspension is dried, XPS detects on the as-prepared surface 35% of carbon. A line shape analysis of the 1s-photoelectrons around 290 eV (C) and 530 eV (O) points to mostly carbohydrate contaminations with some carboxylate and sulfate functionalities, attributed to side products form the synthesis process. Traces of sodium, potassium, and chloride ions were identified in low concentrations (in the order of 2 at.%). The core is crystalline CdS as identified in selected area diffraction (SAD). The $Cd(OH)_2$ passivation layer leads to a sufficiently high zeta potential of −43 mV. The state of agglomeration in the suspension was characterized by analytical ultracentrifugation (AUC). We found that 45% of the QD are well dispersed in water, and the rest are minimally agglomerated to clusters of 2 or 3 QD. Furthermore, transmission electron microscopy (TEM) was used to examine the morphology of the test material in the atmosphere (Fig. 1a and b).

The QD test material was tested for bacteria (aerobic, anaerobic and microaerophilic) and fungi (asco-, basidio and zygomycotic) using agar plate cultures and nucleic acid analysis (amplification of 16S and ITS1/2-rDNA for eubacteria and fungi, respectively). No bacterial or fungal contamination was detected. The endotoxin content was tested using the Limulus Amebocyte Lysate (LAL) Kinetic-QCL Test (Cambrex/Lonza, Walkerville, MD, USA). QD interfere with the detection of endotoxins in this assay (the formation of p-nitroaniline is detected by its absorption at 405 nm U.S. Department of Health, 2000). Therefore QD were removed from the dispersion by ultracentrifugation and only the supernatant was tested. Absorption of potential endotoxins to the QD was checked by spiking the QD dispersion with endotoxin (0.5 EU/mL) prior to centrifugation, and the endotoxin absorption was found to be negligible. The endotoxin content of the QD dispersion was about 2 EU/mL; equivalent to 200 pg/mL LPS. Epstein et al. (1990) showed that up to 20 ng/mL did not affect the proliferation of seven cell lines.

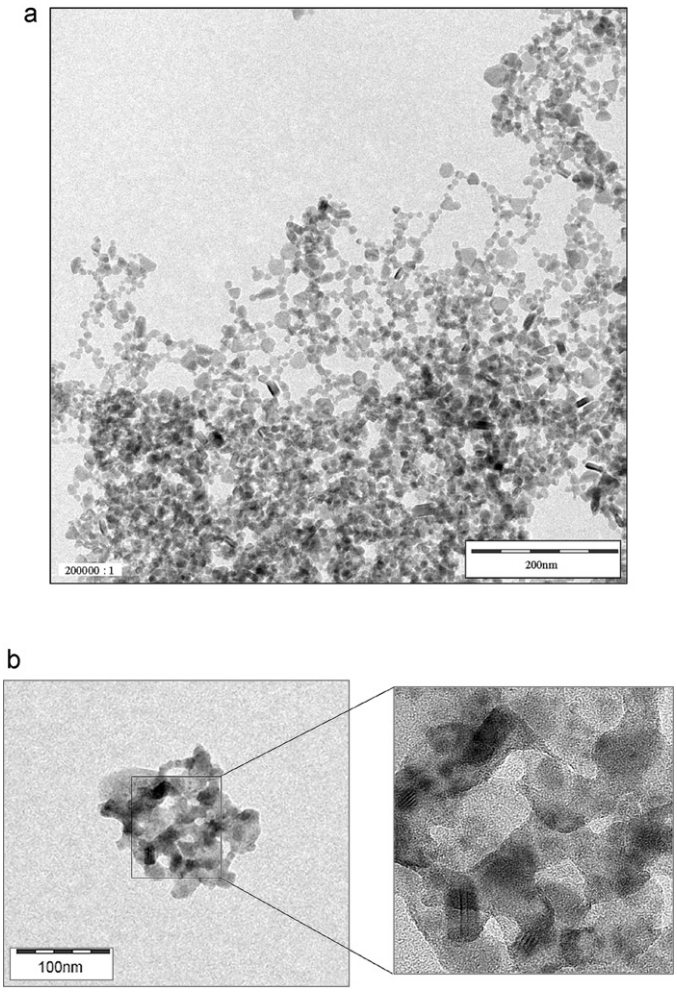

Fig. 1. (a) Morphology of the test material in the atmosphere. TEM of material upon drying (*before* aerosolization). (b) TEM-images of the test material obtained (droplet) from the test atmosphere. High electron density was due to Cd and S containing particles, whereas the ambient phases probably derived from the stabilizing agent of the quantum dot dispersion.

2.2. Animals

Male Wistar rats (Crl:WI); supplied by Charles River (Sulzfeld, Germany), 8–9 weeks old at start of dosing and free from clinical signs of disease, were allocated randomly by weight to the control and test groups. During the exposure, the animals were restrained in glass tubes fixed to the inhalation system. When not exposed, up to 5 animals were housed in 0.2 m^2 polycarbonate cages (TECNIPLAST H-Temp (PSU), Hohenpeissenberg, Germany) with dust-free bedding (Lignocel FS 14 fibers; SNIFF, Soest, Germany) and wooden gnawing blocks (type NGM E-022; supplied by Abedd Lab. and Vet. Service GmbH, Vienna, Austria). The animals' room was air-conditioned with a 12-h light/12-h dark cycle, the temperature ranging from 20 to 24 °C with relative humidity ranging from 30 to 70%. Except during the exposure, certified feed (Kliba GLP rat/mouse maintenance diet meal, Provimi Kliba SA, Kaiseraugst, Switzerland) and tap water (human drinking quality) were available *ad libitum*. The food used in the study was assayed for chemical as well as for microbiological contaminants. The drinking water is regularly assayed for chemical contaminants by the municipal authorities of Frankenthal, Germany, and the Environmental Analytics Water/Steam Monitoring of BASF SE, as well as for the presence of microorganisms. The bedding and enrichment are regularly assayed for contaminants (chlorinated hydrocarbons and heavy metals). All the results of contaminant analyses of diet, bedding, enrichment and drinking water were within limits required for maintenance of laboratory animals. Before start of the exposure period all animals were acclimatized to the inhalation system on 2 consecutive days under conditions comparable to exposure (4–6 h).

2.3. Experimental design

This study was performed in an Association for Assessment and Accreditation of Laboratory Animal Care (AAALAC)-approved laboratory in accordance with the

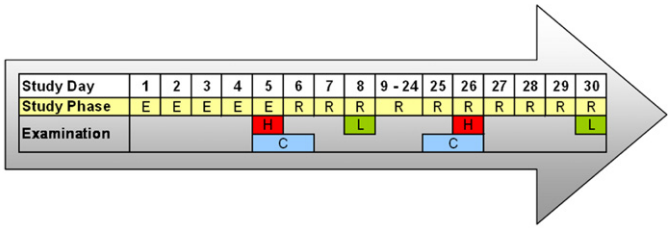

E: Head-nose exposure to aerosols for 6 hours per day on 5 consecutive days

R: Recovery period

H: Histopathological examinations, Organ / tissue preparation for Cd analysis

L: Blood sampling, Lavage

C: Collection of excreta

Fig. 2. Study design.

German Animal Welfare Act, European Council Directive 86/609/EEC, and the OECD Principles of Good Laboratory Practice (OECD, 1981). The study design was based on the OECD Guidelines for Testing of Chemicals, Section 4: Health Effects, No. 412, "Repeated Dose Inhalation Toxicity: 28-day or 14-day Study". Male Wistar rats were head-nose exposed to a liquid aerosol of Cd-based QD for 6 h per day on 5 consecutive days. During the inhalation period the animals were exposed to the technically maximum achievable concentration, which corresponds to 0.52 mg Cd/m^3. The generation and characterization of the aerosol from the nanomaterial as well as the exposure regime and the biological parameters readout have been optimized for nanomaterials (Ma-Hock et al., 2007, 2009). Histological examination of selected organs was performed directly after the last exposure on study day 5 (3 animals per group). In the same animals designated for histopathological examination, TEM was performed (1 control animal and all 3 QD-exposed animals). To identify the particles observed EDX was performed for the lung of one of the three animals examined previously by TEM. Additionally one control and two exposed rats were used for Cd organ burden determinations at each time point. Bronchoalveolar lavage, blood chemistry and hematology were conducted 3 days after last exposure (study day 8; 5 animals per group). To analyze the reversibility or progression of effects, the whole panel of examinations was performed again after a recovery period of 3 weeks.

2.4. Inhalation system (Fig. 2)

The inhalation system used was a 90-L stainless steel cylinder with a cone-shaped inlet and outlet at opposite ends. During exposure, the animals were fixed in glass tubes (attached to the wall of the cylinder) with their snouts projecting into the inhalation chamber. The mean air flow rate through this inhalation system was 6 m^3/h which means a change of air about 67 times per hour. To avoid dilution of the aerosol in the animals' breathing zone with laboratory air, positive pressure was generated inside the inhalation chamber. Additionally, the whole exposure system was kept under exhaust hoods in an air-conditioned room.

2.5. Generation of inhalation atmospheres (Fig. 3)

The generation and characterization of aerosol containing nanoparticles has been optimized and described by Ma-Hock et al. (2007). To generate an inhalable liquid aerosol the test material was fed to a two-component atomizer of stainless steel (Schlick mod. 970) at the inlet of the inhalation chamber. The test substance was supplied by a piston metering pump (Sarstedt DESAGA) with a constant pump rate of 200 mL/h and sprayed with compressed air (pressure: 1.5 bar) into the inhalation system. Test group animals were exposed to the liquid aerosol of the test material, while control group animals were exposed to highly deionized water, sprayed with the same pump rate used for the test group.

Compressed supply and exhausted air flow rate, chamber temperature and humidity were measured three times per exposure.

2.6. Test substance concentration analysis

Real time concentration of the test material in the inhalation chamber was monitored continuously by scattered light photometers (VisGuard, Sigrist-Photometer AG, Switzerland).

Two air samples per exposure were taken next to the animals' breathing zone (probe internal diameter 7 mm) to determine the test atmosphere concentration. A defined volume of sample air (180 L in the test group) was drawn by a vacuum pump across a binder-free glass fiber filter (Macherey-Nagel MN 85/90 BF, diameter 4.7 cm). The concentration of the non-volatile fraction in mg/m^3 was calculated from the difference of the filter weight before and after sampling and drying. Additionally, the same sample filters (one per exposure) were used to analyze the Cd concentration in the test atmosphere using ICP-OES carried out at the Competence Center Analytics, BASF SE, Ludwigshafen, Germany.

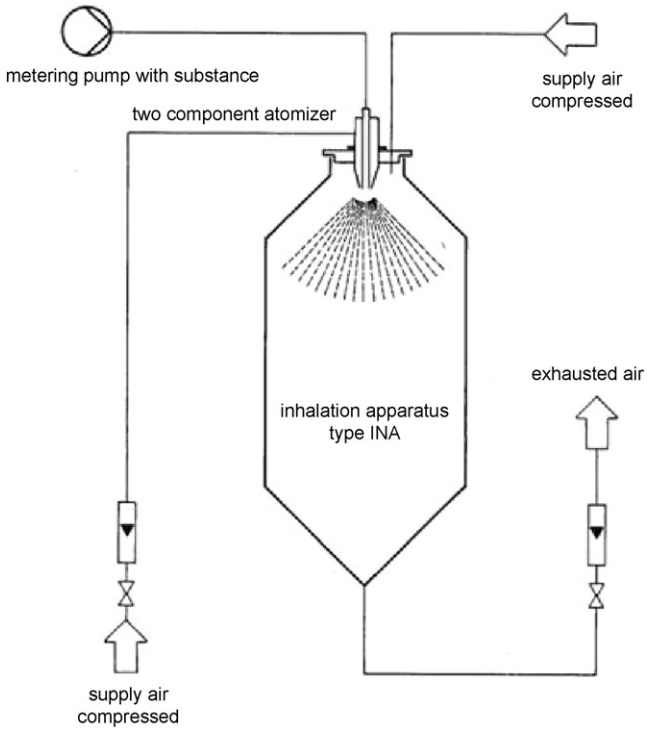

Fig. 3. Generator system.

2.7. Particle size analysis

Samples of the generated test atmosphere were taken for droplet size distribution analysis. A cascade impactor (Sierra Marple 298) was used for droplets down to 0.4 μm (gravimetrical determination, sample volume 45 L). The size of the droplets containing QD was expressed as mass median aerodynamic diameter (MMAD), the calculated aerodynamic diameter which divides the size distribution in half when measured by mass, plus/minus the geometrical standard deviation (GSD) which is the ratio of the estimated 84th to 50th percentile and indicates the broadness of the cumulative drops containing particles size distribution curve. The size distribution of the droplets containing QD was calculated at the Experimental Toxicology and Ecology Department of BASF SE on the basis of mathematical methods for evaluating particle measurements (DIN 66141: *Darstellung von Korngrößenverteilungen* and DIN 66161: *Partikelgrößenanalyse*). In two separate sub-micrometer ranges (5.5–350 nm and 11–1083 nm), the size distribution was measured with a scanning mobility particle sizer (SMPS) which separates the QD containing droplets according to their size which are then counted by a condensation particle counter (Grimm Aerosol Technik GmbH, Ainring, Germany). To assess the morphology of the aerosol droplets, samples for TEM analysis were obtained from the generated atmosphere. It should be emphasized here that water of the aerosol droplets partially evaporates while the droplet is dispersed in dry air and traveling to the rat's nose. This reduces the volume of the droplet and is expected to facilitate agglomeration which was also observed due to water evaporation during sample preparation for the TEM analysis.

2.8. Clinical observations

Clinical observation of the animals was performed three times on exposure days (before, during and after exposure) and once daily during the pre-flow and recovery periods. The body weight of the animals was determined at the beginning of the exposure period and then once weekly and prior to gross necropsy.

2.9. Analysis of Cd content in organs and excreta

On study days 5 and 26, selected organs (brain, kidneys, liver, lungs, mediastinal lymph nodes, and spleen) were taken from 1 control and 2 treated animals per time point, weighed and stored at −80 °C (Table 1). Furthermore, in animals designated for broncho-alveolar lavage (5 animals per group and time point), urine and feces were sampled overnight from study day 5 to 6 and after a recovery period from study day 25 to 26, prior to scheduled lavage on study days 8 and 30. Organ and excrement samples were analyzed for Cd content using ICP-OES at the BASF Competence Center Analytics in Ludwigshafen, Germany.

Table 1
Animal numbers used for each endpoint.

Test performed	Exposure	Number of animals	
		Examination on days 5 or 8	Examination on days 28 or 30
Blood sampling and broncho alveolar lavage[a] also urine and feces sampling	Water aerosol (control)	5	5
	Test substance QD suspension aerosol	5	5
Histopathological examinations (light and transmission electron microscopy)[b]	Water aerosol (control)	3	3
	Test substance QD suspension aerosol	3	3
Organ burden by ICP-OES[b]	Water aerosol (control)	1	1
	Test substance QD suspension aerosol	2	2

[a] Study days 8 and 30.
[b] Study days 5 and 28.

2.10. Histopathology

On study days 5 (after the last exposure) and 26, 3 rats per group were exsanguinated under sodium pentobarbital anesthesia. Selected organs were weighed, fixed in 4% buffered formaldehyde and embedded in paraffin. For histopathology, organ slices (nasal cavity (level I–IV, larynx (level I–III)), trachea with bifurcation, lung, mediastinal and tracheobronchial lymph nodes, kidney) were stained with hematoxylin-eosin and examined by light microscopy.

2.11. Transmission electron microscopy

Animals designated for electron microscopic examination were subjected to deep anesthesia with Isoflo® (Essex GmbH, Munich, Germany). After opening the thorax the animals were sacrificed and fixed by whole-body perfusion using caccodylate buffer as a rinsing solution, followed by perfusion of 5% buffered glutardialdehyde (GAH) as fixation solution. The tissue samples of the lungs were refixed with 2% buffered osmium tetraoxide. The fixed tissue embedded in epoxy resin, semithin sections were made. From appropriate locations ultrathin sections were performed and examined by TEM and EDX.

2.12. Clinical pathology

Blood: In the morning of study days 8 and 30, blood samples were taken from 5 non-fasted animals per group by retroorbital venous plexus puncture under isoflurane anesthesia (Isoba®, Essex GmbH Munich, Germany). The following parameters were determined in EDTA-K3 containing blood with a hematology analyzer (Advia 120, Siemens Diagnostics, Fernwald, Germany): red blood cell counts, hemoglobin, hematocrit, mean corpuscular volume (MCV), mean corpuscular hemoglobin content (MCH), mean corpuscular hemoglobin concentration (MCHC), platelet counts, total white blood cell as well as differential blood cell count. In addition, the following acute phase proteins were determined in serum: haptoglobin (photometric assay based on the preservation of the hemoglobin peroxidase activity (Tridelta Ltd., Maynooth, Ireland) measured with the COBAS Fara (Roche, Basel, Switzerland)); rat α2-macroglobulin (ELISA (Kamiya Biomedical Company, Seattle, USA) measured with a Sunrise MTP Reader, Tecan AG, Switzerland, using the Magellan Software provided by the manufacturer).

Bronchoalveolar lavage fluid (BALF): On days 8 and 30, animals designated for lung lavage (5 animals per group) were sacrificed by exsanguination from the aorta abdominalis and vena cava under Narcoren® anesthesia and the lungs were washed with two instillations of physiologic saline solution (flow rate 12 mL/min; the instillation volume was adjusted to the mean group body weight (2× about 6–8 mL/rat) and mixed prior to analysis).

An automatic analyzer (Hitachi 917; Roche, Mannheim, Germany) was used to measure humoral parameters in the BALF, i.e. total protein (turbidimetric method with benzethonium chloride), lactate dehydrogenase (EC 1.1.1.27; kinetic UV test, 340 nm, 37 °C acc. to IFCC), alkaline phosphatase (EC 3.1.3.1; kinetic color test, 450 nm, 37 °C acc. to IFCC), N-acetyl-β-D-glucosaminidase (EC 3.2.1.30; color test, 580 nm, 37 °C; Yakata et al., 1983) and γ-glutamyltransferase (EC 2.3.2.2, Szasz method (kinetic color test, 415 nm, 37 °C acc. to IFCC)) activities. Total cell counts were determined using a hematology analyzer (Advia 120 Siemens Diagnostics, Fernwald, Germany). Cytocentrifuge preparations were stained according to Wright (Brown, 1993) and evaluated microscopically (Warheit and Hartsky, 1993) for macrophages, polymorph nuclear neutrophils, lymphocytes, monocytes, eosinophils and atypical cells.

Antigens in BALF were measured at Rules-based Medicine Inc., Austin, TX, USA, using xMAP technology (Luminex Corp., Austin, TX, USA) as described previously (Elshal et al., 2006; Fulton et al., 1997; Kettman et al., 1998; Skogstrand et al., 2005; Table 2).

2.13. Lung tissue homogenate

After bronchoalveolar lavage was performed the right lung portion of each animal was resected and stored at −80 °C until lung tissue homogenate preparation: 0.2 g of the main lobe (lobus caudalis dexter) was mixed with 0.8 mL ice-cold tissue protein extraction reagent (T-PER, cat. no. 78510, Pierce Biotechnology, Rockford, IL, USA) containing a complete protease inhibitor cocktail (cat no., 11,873,580,001, Roche, Basel, Switzerland), and homogenized for up to 40 s with an Ultra-Turrax (IKA, Staufen, Germany). The homogenate was centrifuged at 14,000 × *g* and 4 °C for 5 min.

Antigens in lung tissue homogenate were measured at Rules-based Medicine Inc., Austin, TX, USA, using xMAP technology (Luminex Corp., Austin, TX, USA) as mentioned above (Table 2).

2.14. Statistics

Body weights were analyzed by a comparison of the dose group with the control group using the Welch *t*-test (two-sided) for the hypothesis of equal means (Welch, 1947). Humoral parameters in BALF were analyzed by non-parametric one-way analysis using Kruskal–Wallis test (two-sided), and if $p < 0.05$, pair-wise comparison of each dose group with the control group using the Wilcoxon test for the hypothesis of equal medians (Siegel, 1956).

3. Results

3.1. Characterization of test substance and test atmosphere

ICP-OES-Analysis and UV–vis fluorescence spectroscopy resulted in a Cd concentration of 67.0 mg and a sulfur concentration of 13.3 mg/kg test substance.

Real time monitoring with scattered light indicated a constant concentration of the test substance throughout the exposure period. The air flow was also constant within the desired limits. The temperature in the inhalation systems was within the range of 16.4–17.0 °C. Relative humidity was approximately 100% because an aqueous dispersion was sprayed. The mean concentration of the non-volatile fraction of the test item was 4.1 ± 0.5 mg/m^3, measured by gravimetry, and this concentration corresponded to a mean atmospheric Cd concentration of 0.52 mg/m^3 determined by ICP-OES analyses of representative filter samples. Because the QD suspension was used unchanged and also unpurified in the study, the measured Cd concentration could not be used to calculate the concentration of CdS/Cd(OH)$_2$ particles. Size analysis revealed mass median aerodynamic diameters (MMADs) between 1.7 and 2.9 μm with GSD ranging from 6.5 to 4.3 for the droplets containing QD. The calculated mass fractions of droplets below 3 μm aerodynamic size ranged between 51.4 and 62.3%, indicating that a large fraction of the aerosol contained droplets which are respirable for rats. The droplet count concentration and count median diameter are presented in Table 3 with comparable count median diameters of 72.8 (5.5–350 nm) and 78.6 nm (11–1083 nm). Only 2.7% of the total number concentration was between 5.5 and 20 nm (measurement range 5.5–350 nm). These data indicate that the dots were present as agglomerates in the atmosphere. The analysis of the test atmosphere by TEM showed agglomerates between 60 and 100 nm in size, which conforms well to the SMPS analyses.

Table 2
Antigens measured in BALF and lung tissue homogenates.

Abbreviation	Name	Abbreviation	Name
Apo A1	Apolipoprotein A1	IP-10	Interferon-inducible protein-10
CD 40	Cluster of differentiation 40	KC/GRO α	Keratinocyte cytokine/Growth-regulated oncogen-α
CD 40 L	Cluster of differentiation 40 Ligand	LIF	Leukocyte inhibitory factor
CRP	C-reactive protein	Ltn	Lymphotactin
EGF	Epidermal growth factor	MCP-1	Monocyte chemoattractant protein-1
ET-1	Endothelin-1	MCP-3	Monocyte chemoattractant protein-3
	Eotaxin	MCP-5	Monocyte chemoattractant protein-5
Factor VII	Coagulation factor VII	M-CSF	Macrophage colony stimulating factor
bFGF	Basic fibroblast growth factor	MDC	Macrophage-derived chemoattractant
FGF-9	Firoblast growth factor-9	MIP-1α	Macrophage inflammatory protein-1α
	Fibrinogen	MIP-1β	Macrophage inflammatory protein-1β
GCP-2	Granulocyte chemotactic peptid-2	MIP-1γ	Macrophage inflammatory protein-1γ
GM-CSF	Granulocyte-macrophage colony stimulating factor	MIP-2	Macrophage inflammatory protein-2
GST-α	αGluathion-S-transferase	MIP-3β	Macrophage inflammatory protein-3β
	Haptoglobin	MMP-9	Matrix metalloproteinase-9
IFN-γ	Interferon-γ	MPO	Myeloperoxidase
IgA	Immunglobulin A		Myoglobin
IL-1α	Interleukin-1-α	OSM	Oncostatin M
IL-1β	Interleukin-1-β	RANTES	Regulated upon activation, normal T-cell expressed and presumably secreted
IL-2	Interleukin-2	SCF	Stem cell factor
IL-3	Interleukin-3	SAP	Serum Amyloid P
IL-4	Interleukin-4	SGOT	Serum Glutamat-oxalacetat-transaminase
IL-5	Interleukin-5	TIMP-1	Tissue inhibitor of metalloproteinases-1
IL-6	Interleukin-6	TF	Tissue factor
IL-7	Interleukin-7	TNF-α	Tumor necrosis factor-α
IL-10	Interleukin-10	TPO	Thrombopoetin
IL-11	Interleukin-11	VCAM-1	Vascular cellular adhesion molecule-1
IL-12p70	Interleukinfragment-12p70	VEGF	Vascular endothelial growth factor
IL-17	Interleukin-17	vWF	von Willebrand Factor

3.2. Clinical examination

The exposure to CdS/$Cd(OH)_2$ QD did not induce any premature mortalities throughout the study. Furthermore there were neither clinical signs of toxicity nor effects on body weight development.

3.3. Analysis of Cd content in excreta and selected organs

Following the collection period on day 5, Cd content of brain, mediastinal lymph nodes, and spleen was below the detection limit (<0.3 μg per organ). The ICP-OES analysis does not allow the discrimination between Cd particles and Cd ions; thus the total Cd content of tissues (and excreta) is given: Cd was detected in the lungs, liver and kidneys. After a recovery period, the Cd content in the animals' lungs was slightly decreased, whereas in kidneys and liver slightly increased Cd values were measured (Table 4).

Table 3
Characterization of the test atmosphere.

Parameter	Test atmosphere
Measured concentration ± SD [mg/m³]	4.1 ± 0.5
Cd concentration ± SD [mg/m³]	0.52 ± 0.03
MMAD [μm]/GSD	
Measurement 1	1.7/6.5
Measurement 2	2.9/4.3
SMPS with *M*-DMA	
Count concentration of particles [N/cm³]	1,964,118
Count median diameter [nm]/GSD	72.81/1.82
SMPS with *L*-DMA	
Count concentration of particles [N/cm³]	2,485,445
Count median diameter [nm]/GSD	78.59/1.85

Note: Data are mean ± standard deviation unless otherwise indicated. GSD: Geometric standard deviation, the ratio of the estimated 84 percentile to the 50 percentile indicating the slope of the cumulative particle size distribution curve, SMPS: Scanning Mobility Particle Sizer apparatus, DMA: Differential Mobility Analyzer, measurement range of the *L*-DMA is 10.1–1083, measurement range of the *M*-DMA is 5–350 nm.

Analysis of excreta revealed no Cd in urine. In feces Cd content varied widely between the different samples collected directly after exposure (from 18.5 to 74.4 μg/g feces). After 3 weeks of recovery Cd was no longer detectable in feces.

In concurrent control animals exposed to water, Cd was not detected in any samples (all examined organs, urine or feces) at any time point.

3.4. Clinical pathology

There were no effects of treatment on hematology parameters or acute phase protein levels in serum (data not shown). Treatment-related changes were observed in BALF on study day 8 (Table 5): marginally increased total cell and markedly increased neutrophil counts, higher total protein levels, higher enzyme activities (GGT, LDH, ALP, NAG), and higher antigen levels (myeloperoxidase (MPO), monocyte chemoattractant protein (MCP)-1 and -3, macrophage-derived chemoattractant (MDC), granulocyte chemotactic peptide-2 (GCP-2), fibrinogen, macrophage colony stimulating factor (M-CSF), and macrophage inflammatory proteins (MIP-1β, MIP-2)) (Tables 5 and 6). Higher antigen levels (keratinocyte cytokine/growth-regulated oncogen-α (KC/GROα), MDC, and MIP-2) were also recorded in lung tissue homogenates from treated rats (Table 6). Three weeks later, significantly increased neutrophils, higher ALP activities and higher antigen levels (GCP-2, MCP-1, MCP-3, MDC) still persisted in BALF of treated rats albeit at a lower level (Table 5). Higher antigen levels also persisted in lung tissue homogenates from treated rats (KC/GROα, MDC, MIP-2; Table 7).

3.5. Necropsy and histopathology

During necropsy no macroscopic findings were observed in animals investigated either directly after the end of exposure or after the 3-week recovery period. Histopathological examination did not reveal any changes in upper respiratory tract and in kidney.

Table 4
Results of Cd analysis in selected organs.

Animal	Study day 5 (directly after exposure)			Study day 26 (after 3-week recovery)		
	Lung [μg Cd]	Liver [μg Cd]	Kidneys [μg Cd]	Lung [μg Cd]	Liver [μg Cd]	Kidneys [μg Cd]
Control animal	n.d.	n.d.	n.d.	n.d.	n.d.	n.d.
Test animal 1	9.6	1.8	0.4	6.0	2.0	1.4
Test animal 2	10.5	1.3	0.5	8.6	2.1	1.5

Note: Cd content measured by ICP-OES, which does not differentiate between QD particles and Cd ions, merely total Cd contents are given.
n.d., not detected, the detection limit was 0.3 μg Cd per organ.

Histopathological examination of exposed animals directly after treatment revealed a minimal to moderate number of pneumocytes with apoptosis and minimal diffuse infiltration of neutrophils and histiocytes. All these findings were no longer observed after the recovery period.

In the mediastinal and tracheobronchial lymph nodes of two animals of the main group there was a mild to moderate infiltration of histiocytes in the paracortex. After the recovery period two animals showed minimal to moderate granulomas in these lymph nodes.

3.6. Transmission electron microscopy

Numerous electron dense particles, ~10 nm in diameter, were located within phagolysosomes in alveolar macrophages. Performing EDX analysis on these particles, a Cd and S spectrum was observed. These two elements were not seen in the adjacent tissue during EDX analysis (see Fig. 4).

4. Discussion

Rats were exposed by inhalation for 6 h/day on 5 consecutive days to an aerosol of a $CdS(CdOH)_2$ QD aqueous suspension at an average Cd concentration of 0.52 mg/m^3, corresponding to 4.1 mg/m^3 non-volatile fraction. This concentration was the maximum technically achievable concentration under the current test conditions. The Cd concentration detected in the air is the sum of two sources: the main source being the Cd present in the QD the minor source being Cd^{2+} in the aqueous dispersant (10 ± 1 ppm).

The main fraction of the droplets in the aerosol had an aerodynamic size below 3 μm; thus it was respirable for rats and could reach the alveoli. The actual size of the droplets containing QD in the air as determined by SMPS measurement indicated a median diameter ranging between 73 and 79 nm which correlated well with the TEM analyses of the test atmosphere revealing small agglomerates of 60–100 nm size. This would indicate that the QD agglomerated to some extent despite their zeta potential. Agglomeration is to be expected during aerosol generation and examination by TEM: generation of aerosol induces evaporation of water and hence a change of zeta potential of QD; there are also indications that the electrical properties of QD may be altered under pressure (Teisseyre et al., 2006). The consequence of this drying effect under pressure is the observed agglomeration (Figs. 5 and 6).

After the last exposure, Cd was detected in lungs, liver, kidneys and feces but not in urine. The concentration of QD in the lung (approximately 10 μg Cd) at the end of the exposure period indicates a deposition value of 5.3%. Potentially, there are several sources which could account for the systemically measured Cd concentrations: (i) uptake of QD from the lung and subsequent distribution, (ii) uptake of Cd ions from aqueous dispersant or (iii) oral uptake from contaminated fur. First of all, in course of mucociliary clearance the QD deposited in bronchi can be dispatched to pharynx, be swallowed and get into GI tract. We believe this mechanism is the major contributor to the excretion of Cd

Table 5
Absolute values of cell counts, total protein levels, antigens and enzyme activities in BALF on study day 8 (3 days after last exposure) and study day 30 (3 weeks after last exposure) of male Wistar rats treated with QD (n = 5 per group). The antigens are mentioned when their levels exceeded the detection limit, and when they were increased more than 1.5-fold in the dose group on study day 8.

Analyte	Study day 8		Study day 30	
	Control	Exposed to QD	Control	Exposed to QD
Total Cells [count/μL]	36.28	53.09*	28.94	27.17
Eosinophils [count/μL]	0.04	0.31	0	0.06
Lymphocytes [count/μL]	0	0.23	0.07	0.02
Macrophages [count/μL]	35.61	36.80	28.47	21.83
Neutrophils [count/μL]	0.63	15.52*	0.40	5.19*
Atypical cells [count/μL]	0	0.23*	0	0.07
Total Protein [mg/L]	32	64*	48	48
GGT [nkat/L]	18	38*	18	23
LDH [μkat/L]	0.19	0.39*	0.25	0.25
ALP [μkat/L]	0.26	0.60*	0.47	0.67
NAG [nkat/L]	17	26*	17	19
MCP-1 [pg/mL]	1.9	13.7*	1.9	4.92**
MCP-3 [pg/mL]	4.1	23.8*	4.2	8.08*
M-CSF [ng/mL]	0.041	0.069*	0.040	0.050
MDC [pg/mL]	16.75	87.25*	21.0	55.4*
MIP-1β [pg/mL]	19.5	35.5*	22.4	26.0
MIP-2 [pg/mL]	6.13	10.08*	6.26	7.84
GCP-2 [ng/mL]	0.011	0.038*	0.011	0.039**
MPO [ng/mL]	0.17	6.88*	0.29	0.61
Fibrinogen [μg/mL]	1.13	2.8	1.92	1.08*

GGT: γ-glutamyl-transferase; LDH: lactate dehydrogenase; ALP: alkaline phosphatase; NAG: β-N-acetyl glucosaminidase; GCP-2: granulocyte chemotactic peptide-2; MCP: monocyte chemoattractant protein; M-CSF: macrophage colony stimulating factor; MDC: macrophage-derived chemoattractant; MIP: acrophage inflammatory protein; MPO: myeloperoxidase; two-sided Wilcoxon test: *$p \leq 0.05$; **$p \leq 0.01$.

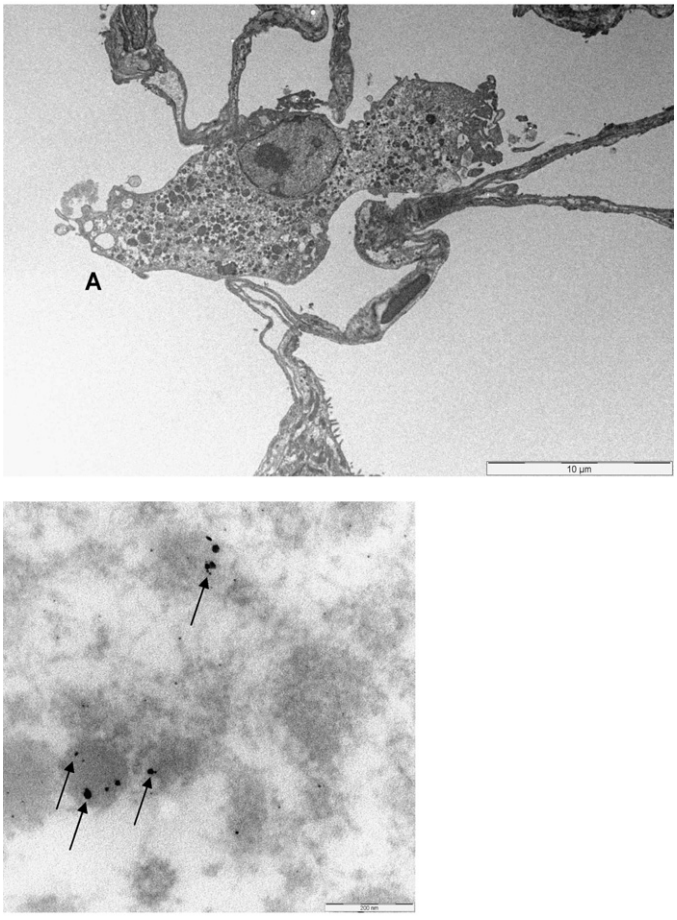

Fig. 4. TEM images of the lung. (a) Alveolar macrophage (A) containing numerous moderate electron dense phagolysosomes within the cytoplasm. (b) Close up of (a): electron dense, approx. 10 nm in diameter particles (quantum dots) mainly locates within phagolysosomes of alveolar macrophages (arrows).

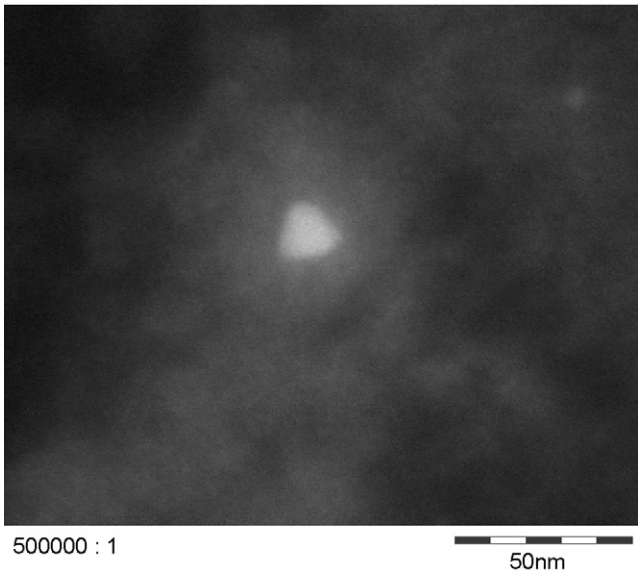

Fig. 5. HAADF STEM. High Angle Annular Dark Field – Scanning Transmission Electron Microscopy (AADF STEM). Compact areas (e.g. high Cd content) appear lighter.

Table 6
Changes (fold of control) in mean total cell counts, total protein levels, antigens and enzyme activities in BALF.

Analyte	Study day 8	Study day 30
Total cells	1.5*	0.9
Eosinophils	7.8	+
Lymphocytes	+	0.3
Macrophages	1.0	0.8
Neutrophils	24.6*	13.0*
Atypical cells	*+	+
Total protein	2.0*	1.0
GGT	2.1*	1.3
LDH	2.1*	1.0
ALP	2.3*	1.4
NAG	1.5*	1.1
MCP-1	7.2*	2.5**
MCP-3	5.8*	1.9*
M-CSF	1.7*	1.3
MDC	5.2*	2.6*
MIP-1β	1.8*	1.2
MIP-2	1.6*	1.3
GCP-2	3.6*	3.5**
MIP-1β	1.8*	1.2
MIP-2	1.6*	1.3
MPO	40.4*	2.1
Fibrinogen	2.5*	0.6*

Note: Changes in BALF are indicted as *x*-fold of concurrent control. Analysis of BALF of male Wistar rats treated with QD ($n=5$ per group) was performed on study day 8 (3 days after last exposure) and study day 30 (3 weeks after last exposure). Antigens are mentioned when their levels exceeded the detection limit, and when they were increased more than 1.5-fold in the dose group on study day 8. GGT: γ-glutamyl-transferase; LDH: lactate dehydrogenase; ALP: alkaline phosphatase; NAG: β-N-acetyl glucosaminidase; GCP-2: granulocyte chemotactic peptide-2; MCP: monocyte chemoattractant protein; M-CSF: macrophage colony stimulating factor; MDC: macrophage-derived chemoattractant; MIP: macrophage inflammatory protein; MPO: myeloperoxidase; two-sided Wilcoxon test: $^{*}p \leq 0.05$; $^{**}p \leq 0.01$; + increase could not be calculated because of a zero value in controls.

in feces. Further, Cd^{2+} in the QD dispersant may become systemically available. In addition, grooming of contaminated fur may also contribute to the oral uptake of QD. Although the inhalation study was performed using head-nose only equipment, the size of the QD or their agglomerates is such that passage along the head-nose equipment to the fur (and subsequent grooming of the fur after the animals had been transferred to their home cages) cannot be excluded. QD present in the nose and mouth region (which were directly exposed) may have moved down the GI tract. Taking into account the likelihood of QD passage through the G.I. tract their stability at different pH values is of importance. Stability of QDs during preparation, with pH values between 6 and 8 is given. Additional analysis demonstrated that colloidal quantum dots maintained their stability until a pH of 5.2. For pH values below 5.2, the particles start to dissolve and release Cd^{2+} ions. Taking into account the average pH values in rat stomach (ranging between pH 3.1 and 5.1), release of Cd^{2+} ions in the stomach cannot be excluded. This conclusion is in line

Table 7
Changes in antigen levels in lung tissue homogenates.

Analyte	Study day 8	Study day 30
MDC	2.8*	1.5*
MIP-2	2.0*	2.0**
KC/GROα	6.8*	5.1**

Note: Changes in antigen levels in lung tissue homogenates are indicted as *x*-fold of concurrent control. Analysis of antigen levels in lung tissue homogenates of male Wistar rats treated with QD ($n=5$ per group) was performed on study day 8 (3 days after last exposure) and study day 30 (3 weeks after last exposure). The antigens are mentioned when their levels exceeded the detection limit, and when they were increased more than 1.5-fold in the dose group on study day 8. KC/GROα: keratinocyte cytokine/growth-regulated oncogen-α; MDC: macrophage-derived chemoattractant; MIP: macrophage inflammatory protein; two-sided Wilcoxon test: $^{*}p \leq 0.05$; $^{**}p \leq 0.01$.

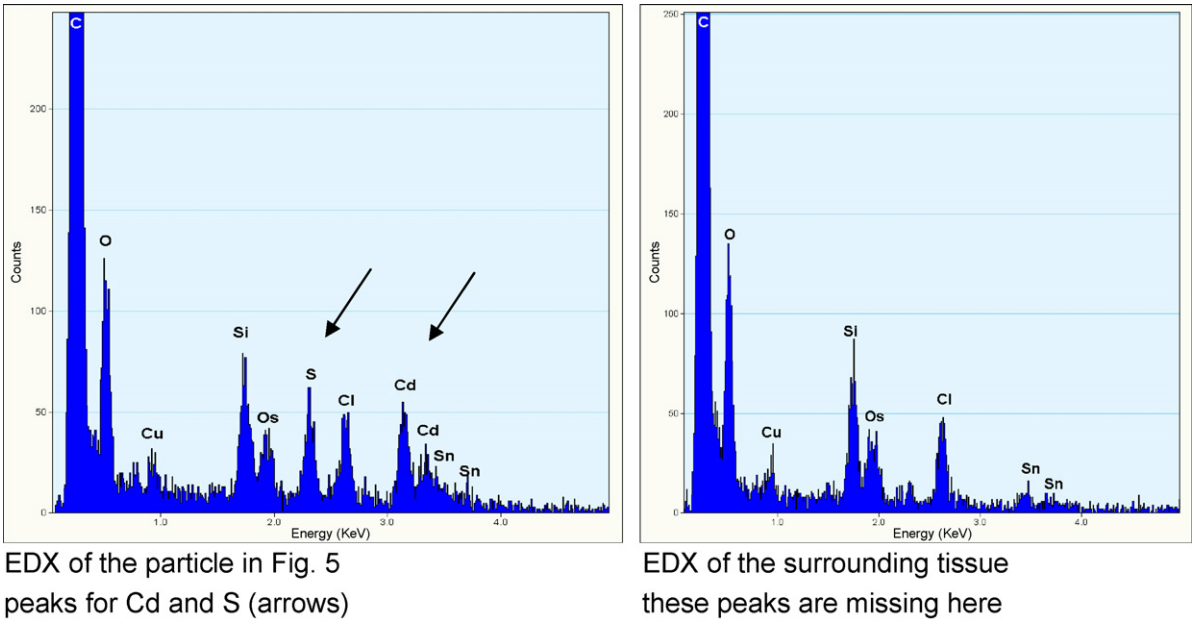

Fig. 6. Energy dispersive X-ray spectroscopy (EDX).

with the observations made by Karabanovas et al. (2008). After a recovery period of 3 weeks, Cd was no longer detectable in feces, but persisted in lungs, liver and kidneys. The concentrations in the lung after the last exposure on study day 5 were rather low, relative to the concentrations found in the feces at that time, but the material in the lung persisted without a profound reduction. This would suggest that the Cd detected in the lungs was associated with the QD, rather than free Cd ions from the suspension because the latter would not be expected to persist for 3 weeks. Cd found in the liver and kidney may be be associated with the QD. This would be in line with results reported by Chen et al. (2008), who noted that the highest concentrations of QD were observed in the liver and the kidneys following i.v. injections in rats. The route of entry of the QD in our study cannot be determined with certainty as both oral as well as inhalation uptake appear to be possible. The absence of Cd in the urine after the last exposure on study day 5 does not necessarily indicate that there was no elimination of Cd through the urine during the exposure period, since rapid urine was not collected during the exposure period in the present study design. Chen et al. (2008) noted that following i.v. injection of QD elimination through the feces was more pronounced than via urine. The results of our study indicate that there is very little elimination of QD after they have become systemically available. Liver and kidney Cd concentrations appear rather within the 3 weeks after the last exposure. This observation is in line with the results of Lin et al. (2008), who noted that following i.v. injection of CdSeTe core QD in mice, the QD accumulated in spleen, liver and kidneys for at least 28 days and were only gradually eliminated over 6 months.

There were no obvious signs of toxicity during the exposure in any of the animals investigated. However, 3 days after last exposure (study day 8), an inflammatory reaction was observed in the lungs of treated rats characterized by higher counts of neutrophils and atypical cells (most probably activated macrophages) in BALF. Sessile cells in the lungs (e.g. endothelial cells, smooth muscle cells, fibrocytes) affected by the exposure must have induced a release of mediators to attract neutrophils and monocytes/macrophages into lung tissue as indicated by increased MCP-1, MCP-3, GCP-2 and KC/GROα values. This was accompanied by an increase of MPO levels in BALF derived from neutrophils, higher MDC levels in the lung tissue derived from activated monocytes/macrophages, and higher acute phase protein levels (i.e. fibrinogen and CRP) due to lung capillary leakage. The inflammatory reaction was also observed during light microscopy examination in the form of an infiltration of neutrophils and histiocytes. In addition, minimal to slight numbers of apoptotic pneumocytes were observed. This is most likely a consequence of the inflammatory reaction and the released mediators. Thus, the overall acute response of inhalation exposure of rats to QD was limited to a moderate inflammatory effect in the lung. This type of response is commonly seen following inhalation exposure to nanomaterials (van Ravenzwaay et al., 2009). Partial regression of the inflammatory response was seen after a 3-week recovery period. Although regression of effects after cessation of exposure is usual, it should be noted that the Cd concentrations in the lung did not decline in an appreciable way. This could possibly indicate an adaptation of the lungs to the presence of QD. In the draining lymph nodes of the lung (tracheobronchial and mediastinal) an increase in macrophages was observed directly after cessation of the treatment. After the recovery period these infiltrations formed granulomas. This is an effect often observed when substances are inhaled which cannot easily be processed (Kumar et al., 2010).

Electron microscopy of the lungs showed several electron-dense particles in the lungs and particularly alveolar macrophages of animals exposed to QD but not in control animals. The EDX analysis on particles found in the lung demonstrated a Cd and S spectrum. As these two elements were not seen in the adjacent tissue in the EDX analysis, it can be concluded that these particles are QD and that following lung exposure alveolar macrophages are capable of phagocytoses of QD.

There were small amount Cd found in kidney, which increased very slightly over the post-exposure observation period. Histological examination of kidney did not reveal any morphological abnormalities. This finding is in line with a feeding study in rat (Mitsumori et al., 1998): only high concentration of >200 ppm in diet, corresponding to 104–252 μg/g wet kidney, caused renal dysfunction after 2 months. Human autopsy studies showed a maximum tolerable kidney burden of 50 μg/g wet tissue to avoid any malfunction (Miller et al., 1976; Spickett and Lazner, 1979).

Overall, the results of this inhalation study with QD consisting of a CdS core surrounded by a $Cd(OH)_2$ shell (i.e. non-functionalized

QD) indicate a moderate toxicity. The QD-induced toxicity is limited to an inflammatory response in the lungs. As noted above this type of response is common for most insoluble particles that do not break down easily. Although there are very few reports on the *in vivo* toxicity of QD, our results appear to be in line with the lack of appreciable systemic toxicity following injection of CdSe (core)–ZnS (shell) QD in rats reported by Hauck et al. (2010). The absence of systemic effects of QD in *in vivo* studies reported at this time, however, does not indicate that these materials are without risk. First of all there is a clear lack of studies of prolonged duration, e.g. up to 90 days. Secondly, QD with a Cd core have the potential to release Cd and formulations prepared with such QD will also have a certain concentration of Cd ions. Pelley et al. (2009) reported that minimizing the presence of free Cd ions in QD preparations seems to reduce the toxicity of QD. This, however, was based mainly on the evaluation of *in vitro* assays. In a review of cytotoxicity studies with different coated and uncoated Cd-based QD, Rzigalinski and Strobl (2009) note that a primary source of (*in vitro*) QD toxicity results from Cd residing in the QD core. Uncoated QD have been associated with cytotoxic effects similar to those resulting from Cd toxicity and/or oxidative stress. Coating with ZnS reduced the concentration of free Cd ions and also reduced apoptosis in the *in vitro* assay.

Several reports indicate that QD have a rather low rate of transfer through cellular barriers such as the skin (Gopee et al., 2009; Ryman-Rasmussen et al., 2006) and through a monolayer of primary isolated rat alveolar cells (Geys et al., 2009). Taking all available data into account, it would seem that the toxicity of Cd-based QD could be described by the following points: First, QD do not penetrate barriers such as skin and lung, thus systemic availability is rather low and consequently systemic toxicity is also low or absent (in short-term studies). Second, short-term inhalation toxicity of QD is dominated by local inflammatory effects in the lungs. Third, because of the presence of free Cd ions in QD formulations and the potential release of Cd ions from the core of the QD, subchronic and chronic toxicity of QD may be dominated by free Cd ions. Present methodologies and technologies appear to be sufficient to perform a risk assessment, provided that robust *in vivo* data are available.

Conflict of interest statement

The authors declare that there is no conflict of interest.

Acknowledgements

The authors wish to thank Elke Wittmer, Ernst Bohrer, Stefan Rath, Sarah Koppenhagen, Annette Knecht, Sabine Löffler, Irmgard Weber, Jeanette Vogt, Inta Kögel, Vanessa Seel and Ulrich Flörchinger for their excellent technical assistance in performing the inhalation study, the clinical and histopathological examinations and electron microscopy. We thank Dr. Jürgen Schnekenburger, Medizinische Klinik und Poliklinik B and Prof. Dr. med. Karsten Becker (Institut für Medizinische Mikrobiologie des Universitätsklinikums Münster, Germany) for performing the microbiological analysis.

References

Brown, A.B. (Ed.), 1993. Haematology: Principles and Procedures. , 6th edition. Lea & Febiger, Philadelphia, p. 101.

Brown, D.M., Wilson, M.R., MacNee, W., Stone, V., Donaldson, K., 2001. Size-dependent proinflammatory effects of ultrafine polystyrene particles: a role for surface area and oxidative stress in the enhanced activity of ultrafines. Toxicol. Appl. Pharmacol. 175, 191–199.

Chen, Z., Chen, H., Meng, H., Xing, G., Gao, X., Sun, B., Shi, X., Yuan, H., Zhang, C., Liu, R., Zhao, F., Zhao, Y., Fang X, 2008. Bio-distribution and metabolic paths of silica coated CdSeS quantum dots. Toxicol. Appl. Pharmacol. 230, 364–371.

Dailey, L.A, Jekel, N., Fink, L., Gessler, T., Schmehl, T., Wittmar, et al., 2006. Investigation of the proinflammatory potential of biodegradable nanomaterial drug delivery systems in the lung. Toxicol. Appl. Pharmacol. 215, 100–108.

Elshal, M.F., McCoy Jr., J.P., 2006. Multiplex bead array assays: performance evaluation and comparison of sensitivity to ELISA. Methods 38, 317–323.

Epstein, J., Lee, M.M., Kelly, C.E., Donahue, P.K., 1990. Effect of *E. coli* endotoxin on mammalian cell growth and recombinant protein production. In Vitro Cell. Dev. Biol. 26, 1121–1122.

Farias, P.M.A., Santos, B.S., Menezes, F.D., Ferreira, R., Fontes, A., Carvalho, H.F., Romão, L., Moura-Neto, V., Amaral, J.C.O.F., Lorenzato, F.R.B., 2006. Quantum dots as fluorescent bio-labels in cancer diagnoistic. Phys. Status Solidi (C), 4001–4008.

Fulton, R.J., McDade, R.L., Smith, P.L., Kienker, L.J., Kettman Jr., J.R., 1997. Advanced multiplexed analysis with the FlowMetrix™ system. Clin. Chem. 43, 1749–1756.

Gao, X., Cui, Y., Levenson, R.M., Chung, L.W.K., Nie, S., 2004. In vivo cancer targeting and imaging with semiconductor quantum dots. Nat. Biotechnol. 22, 969–976.

Geys, J., De Vos, R., Nemery, B., Hoet, P.H.M., 2009. In vitro translocation of quantum dots and influence of oxidative stress. Am. J. Physiol. Lung Cell Mol. Physiol. 297, 903–911.

Gilmour, P.S., Ziesenis, A., Morrison, E.R., Vickers, M.A., Drost, E.M., Ford, J., et al., 2004. Pulmonary and systemic effects of short-term inhalation exposure to ultrafine carbon black particles. Toxicol. Appl. Pharmacol. 195, 35–44.

Gopee, N.V., Roberts, D.W., Webb, P., Cozart, C.R., Siitonen, P.H., Latendresse, J.R., Warbitton, A.R., Yu, W.W., Colvin, V.L., Walker, N.J., Howard, P.C., 2009. Quantitative determination of skin penetration of PEG-coated CdSe quantum dots in dermabraded but not intact SKH-1 haitless mouse skin. Toxicol. Sci. 111, 37–48.

Hardman, R., 2006. A toxicologic review of quantum dots; toxicity depends on physicochemical and environmental factors. Environ. Health Perspect. 114, 165–172.

Hauck, T.S., Anderson, R.E., Fischer, H.C., Newbigging, S., Chan, W.C.W., 2010. In vivo quantum dot toxicity assessment. Small 1, 138–144.

Kettman, J.R., Davies, T., Chandler, D., Oliver, K.G., Fulton, R.J., 1998. Classification and properties of 64 multiplexed microsphere sets. Cytometry 33, 234–243.

Karabanovas, V., Zakarevicius, E., Sukackaite, A., Streckyte, G., Rotomskis, R., 2008. Examination of the stability of hydrophobics (CdSe)ZnS quantum dots in the digestive tract of rats. Photochem. Photobiol. Sci. 7, 725–729.

Kreyling, W.G., Semmler, M., Erbe, F., Mayer, P., Takenaka, S., Schulz, H., Oberdörster, G., Ziesenis, A., 2002. Translocation of ultrafine insoluble iridium particles from lung epithelium to extrapulmonary organs is size dependent but very low. J. Toxicol. Environ. Health A 65, 1513–1530.

Kumar, V., Abbas, A.K., Fausto, N., Aster, J.C., 2010. Acute and chronic inflammation. In: Kumar, V., Abbas, A.K., Fausto, N., Aster, J.C. (Eds.), Robbins and Cotran Pathologic Basis of Disease. Saunders Elsevier, Philadelphia.

Landsiedel, R., Ma-Hock, L., Kroll, A., Hahn, D., Schnekenburger, J., Wiench, K., Wohlleben, W., 2010. Testing metal-oxide nanomaterials for human safety. Adv. Mater. 22, 2601–2627.

Lin, P., Chen, J., Chang, L., Wu, J., Redding, L., Chang, H., Yeh, T., Yang, C.S., Tsai, M., Wang, H., Kuo, Y., Yang, R.S.H., 2008. Computational and ultrastructural toxicology of a nanoparticle, quantum dot 705 in mice. Environ. Sci. Technol. 42, 6264–6270.

Ma-Hock, L., Gamer, A.O., Landsiedel, R., Leibold, E., Frechen, T., Sens, B., Linsenbühler, M., van Ravenzwaay, B., 2007. Generation and characterization of test atmospheres with nanomaterials. Inhal. Toxicol. 19, 833–848.

Ma-Hock, L., Burkhardt, S., Strauss, V., Gamer, A.O., Wiench, K., van Ravenzwaay, B., Landsiedel, R., 2009. Development of a short-term inhalation test in the rat using nano-titanium dioxide as a model substance. Inhal. Toxicol. 21, 102–118.

Medina, C., Santos-Martinez, M.J., Radomski, A., Corrigan, O.I., Radomski, M.W., 2007. Nanoparticles: pharmacological and toxicological significance. Br. J. Pharmacol. 150, 552–558.

Miller, G.J., Wylie, M.J., McKeown, D., 1976. Cadmium exposure and renal accumulation in an Australian urban population. Med. J. Aust. 1, 20–23.

Mitsumori, K., Shibutani, M., Sato, S., Onodera, H., Nakagawa, J., Hayashi, Y., Ando, M., 1998. Relationship between the development of hepato-renal toxicity and cadmium accumulation in rats given minimum to large amounts of cadmium chloride in the long-term: preliminary study. Arch. Toxicol. 72, 545–552.

Oberdörster, G., Sharp, Z., Atudorei, V., Elder, A., Gelein, R., Kreyling, W., Cox, C., 2004. Translocation of inhaled ultrafine particles to the brain. Inhal. Toxicol. 16 (6–7), 437–445.

Oberdörster, G., Oberdörster, E., Oberdörster, J., 2005. Nanotoxicology: an emerging discipline evolving from studies of ultrafine particles. Environ. Health Perspect. 113, 823–839.

OECD Principles of Good Laboratory Practice, Paris, 1981.

Siegel, S., 1956. Non-Parametric Statistics for the Behavioural Sciences. McGraw-Hill, New York.

Pelley, J.L., Abdallah, S.D., Saner, M.A., 2009. State of academic knowledge on toxicity and biological fate of quantum dots. Toxicol. Sci. 112, 276–296.

Powell, M.C., Kanarek, M.S., 2006. Nanomaterial health effects. Part 1. Background and current knowledge. Wis. Med. J. 105, 16–20.

Ryman-Rasmussen, J.P., Rivière, J.E., Monteiro-Reviere, N.A., 2006. Penetration of intact skin by quantum dots with diverse physicochemical properties. Toxicol. Sci. 91, 159–165.

Rzigalinski, B.A., Strobl, J.S., 2009. Cadmium containing nanoparticles: perspective on pharmacology and toxicology of quantum dots. Toxicol. Appl. Pharmacol. 238, 280–288.

Skogstrand, K., Thorsen, P., Norgaard-Pedersen, B., Schendel, D.E., Sorensen, L.C., Hougaard, D.M., 2005. Simultaneous measurement of 25 inflammatory markers

and neurotrophins in neonatal dried blood spots by immunoassay with xMAP technology. Clin. Chem. 51, 1854–1866.
Spickett, J.T., Lazner, J., 1979. Cadmium concentrations in human kidney and liver tissues from Western Australia. Bull. Environ. Contam. Toxicol. 23, 627–630.
Teisseyre, H., Suski, T., Lepkowski, S.P., Perlin, P., Jurczak, G., Dluzewski, P., Daudin, B., Granjean, N., 2006. Strong electric field and nonuniformity effects in GaN/AlN quantum dots revealed by high pressure studies. Appl. Phys. Lett. 89, 051902-1–051902-3.
Thomas, K., Sayre, P., 2004. Research strategies for safety evaluation of nanomaterials. Part I. Evaluating the human health implications of exposure to nanoscale materials. Toxicol. Sci. 87, 316–321.
U.S. Department of Health and Human Services Food and Drug Administration, 2000. Guideline on Validation of the Limulus Amebocyte Lysate Test as an End-Product Endotoxin Test for Human and Animal Pareteral Drugs, Biological Products, and Medical Devices.
van Ravenzwaay, B., Landsiedel, R., Fabian, E., Burkhardt, S., Strauss, V., Ma-Hock, L., 2009. Comparing fate and effect of three particles of different surface properties: nano-TiO_2, pigmentary TiO_2 and quartz. Toxicol. Lett. 186, 152–159.
Warheit, D.B., Hartsky, M.A., 1993. Role of alveolar macrophage chemotaxis and phagocytocis in pulmonary clearance responses to inhaled particles: comparisons among rodent species. Microsc. Res. Tech. 26, 412–422.
Welch, B.L., 1947. The generalization of Student's problem when several different population valiances are involved. Biometrika 34, 28–35.
Yakata, M., Sugita, O., Sakai, T., Uchiyama, K., Wada, K., 1983. Urinary enzyme determination and its clinical significance C.Enzyme derived from the kidney tubular epithelium-N-acetyl-beta-D-glucosaminidase. 4. Preclinical evaluation of the urinary NAG activity and changes in renal diseases. Rinsho Byori 56, 90–101.